

---

# Simple Quantification of Skeletal Muscle Glucose Utilization by Static $^{18}\text{F}$ -FDG PET

Ikuo Yokoyama, MD<sup>1</sup>; Yusuke Inoue, MD<sup>2</sup>; Toshiyuki Moritan, MD<sup>1</sup>; Kuni Ohtomo, MD<sup>2</sup>; and Ryozo Nagai, MD<sup>1</sup>

<sup>1</sup>Department of Cardiovascular Medicine, Graduate School of Medicine, University of Tokyo, Tokyo, Japan; and

<sup>2</sup>Department of Radiology, Graduate School of Medicine, University of Tokyo, Tokyo, Japan

---

Skeletal muscle glucose utilization (SMGU) can be measured by dynamic PET imaging with  $^{18}\text{F}$ -FDG to characterize insulin resistance. The aim of this study was to determine the validity of simple methods to quantify SMGU by static PET imaging.

**Methods:** Ten patients underwent dynamic  $^{18}\text{F}$ -FDG PET of the femoral region during hyperinsulinemic euglycemic clamping. SMGU was determined by Patlak graphical analysis using data from dynamic imaging with frequent arterial blood sampling. Standardized uptake values (SUVs) were calculated at 45 and 55 min after tracer injection. Skeletal muscle-to-background ratio (SM/B ratio), tissue count divided by venous plasma activity, was also computed at 45 and 55 min. These simple indices were compared by linear regression with the SMGU measured as above, and an estimated SMGU was obtained using the regression equation thus generated, together with a simple index. **Results:** SMGU was highly correlated with SUVs ( $r = 0.941$  at 45 min,  $r = 0.951$  at 55 min) and SM/B ratios ( $r = 0.968$  at 45 min,  $r = 0.984$  at 55 min). Although SMGU was almost proportional to SM/B ratios, the  $y$ -intercepts of the regression lines for SUVs significantly differed from zero. The residual in estimating SMGU using the regression equation was marginally smaller for SM/B ratios than for SUVs and for indices at 55 min than at 45 min, but these differences did not reach statistical significance. Correction for plasma glucose level slightly elevated the correlation coefficients between SMGU and these simple indices. **Conclusion:** It is proposed that the simple quantitative indices, SUV and the SM/B ratio, are reliable indicators of SMGU during hyperinsulinemic euglycemic clamping. Static imaging with or without a single venous blood sampling may therefore be able to replace dynamic imaging with frequent arterial blood sampling, offering substantially greater convenience in evaluating insulin resistance.

**Key Words:** skeletal muscle; glucose utilization; insulin resistance;  $^{18}\text{F}$ -FDG; PET

**J Nucl Med 2003; 44:1592–1598**

---

**I**nsulin resistance is defined as a decreased glucose utilization response to the stimulatory effect of insulin. It is widely accepted that insulin resistance plays an important

role in the development of ischemic heart disease as well as noninsulin-dependent diabetes mellitus (NIDDM) (1), hypertriglyceridemia (2–4), essential hypertension (5), and other diseases. Because insulin resistance was found to be closely related to the occurrence of coronary artery disease in persons with common underlying coronary risk factors (6,7), investigation of the pathophysiology of and therapeutic strategies for insulin resistance is important for the early prevention of coronary artery disease. Several factors, including impaired skeletal muscle glucose utilization (SMGU) (1), reduced peripheral blood flow (8), and altered fatty tissue metabolism (9,10), have been shown to contribute to insulin resistance. Among these factors, SMGU is thought to be the most important in determining whole-body insulin resistance because it can account for approximately 70%–80% of the whole-body glucose disposal rate (GDR) in normal humans. However, due to technical difficulties, the percentage of SMGU that would contribute to the whole-body GDR in several diseases with whole-body insulin resistance has not been determined. In addition, it is important to distinguish the effects of skeletal muscle glucose metabolism and other factors separately for a much more precise understanding of insulin resistance syndrome in subjects with coronary risk factors.

PET with  $^{18}\text{F}$ -FDG allows the measurement of SMGU *in vivo* (5,11–21). Unlike the whole-body GDR, PET provides an index of regional insulin resistance. Sequential measurement of myocardial glucose utilization (MGU) and SMGU has been reported using a single injection of  $^{18}\text{F}$ -FDG (5,11,20). It is possible that glucose utilization varies between skeletal muscle and myocardium and among skeletal muscles of different compositions.  $^{18}\text{F}$ -FDG PET has the potential to provide detailed insights into the pathophysiology of insulin resistance in clinical settings.

In previous studies, dynamic imaging was performed to evaluate skeletal muscle insulin resistance by  $^{18}\text{F}$ -FDG PET (5,11–20). A 3-compartment model has been used to successfully describe the kinetics of  $^{18}\text{F}$ -FDG in human skeletal muscle (21), like that in the brain. Because dephosphorylation of  $^{18}\text{F}$ -FDG-6-phosphate is negligible in skeletal muscle (22), SMGU can be calculated by Patlak graphical analysis of the acquired dynamic data (23). However, dynamic PET imaging is time-consuming and represents a

---

Received Feb. 10, 2003; revision accepted Jun. 13, 2003.

For correspondence or reprints contact: Ikuo Yokoyama, MD, Department of Cardiovascular Medicine, Graduate School of Medicine, University of Tokyo, 7-3-1 Hongo, Bunkyo-ku, Tokyo 113-8655, Japan.

E-mail: yokochan-tyk@umin.ac.jp

substantial burden for both the patient and the PET laboratory. Patient movement during the imaging process may degrade the acquired data, which is a serious problem, especially in estimating SMGU of the extremities. In oncology,  $^{18}\text{F}$ -FDG uptake in the target region is often estimated by static imaging instead of dynamic imaging. The standardized uptake value (SUV) is calculated from tissue counts on static images, injected dose, and body weight, and its utility is well accepted as an indicator of  $^{18}\text{F}$ -FDG uptake in clinical PET studies (24). Use of the SUV has also been reported for the evaluation of skeletal muscle activity in runners (25); however, it has not been validated as an indicator of SMGU. A similar index, the  $^{18}\text{F}$ -FDG uptake index, was described in cardiology and shown to correlate with MGU (26). The myocardium-to-background ratio (M/B ratio) is another simple index of MGU and is derived from static imaging and a single venous blood sampling (27). Substituting static imaging for dynamic imaging increases convenience and appears to facilitate the sequential assessments of glucose utilization in different regions. In this study, we performed dynamic  $^{18}\text{F}$ -FDG PET of the femoral region with frequent arterial blood sampling to calculate SMGU. The SUV and the skeletal muscle-to-background ratio (SM/B ratio), an analog of the M/B ratio, were defined as simple indices of  $^{18}\text{F}$ -FDG uptake and compared with SMGU. The aim of the study was to examine the validity of simple quantification of SMGU by static  $^{18}\text{F}$ -FDG PET.

## MATERIALS AND METHODS

### Subjects

$^{18}\text{F}$ -FDG PET during hyperinsulinemic euglycemic clamping was performed in 11 patients to evaluate SMGU of the femoral region. They were selected based on the fact that they had diseases with the possibility of associated insulin resistance, and no other specific inclusion criteria were used. One patient was excluded from the analysis because of considerable body movement during the PET imaging. Consequently, 10 patients participated in the study (3 women, 7 men; age range, 27–77 y; mean age,  $57.8 \pm 18.2$  y). Four had NIDDM, 2 hyperlipidemia, 3 both NIDDM and hyperlipidemia, and 1 had hypertension. The general characteristics of study subjects are summarized in Table 1. The investigative nature of the study was fully explained to each patient before informed consent was obtained. The University of Tokyo's Human Subject Protection Committee approved the study protocol.

### PET

$^{18}\text{F}$  was synthesized using the Cypris 370 cyclotron (Sumitomo JYUKI Industries, Ltd.), and  $^{18}\text{F}$ -FDG was synthesized with an automated system based on the method reported by Ehrenkauffer et al. (28). Radiochemical purity was >95%. Skeletal muscle  $^{18}\text{F}$ -FDG images were obtained using a Headtome IV PET scanner (Shimadzu Corp.). This PET scanner has 7 imaging planes; in-plane resolution is 4.5 mm at full width at half maximum (FWHM), and the  $z$ -axial resolution is 9.5 mm at FWHM. Effective in-plane resolution was 7 mm after using a smoothing filter. The sensitivities of the Headtome IV scanners are 378 and 649 kcps (kBq/mL) for direct and cross planes, respectively.

**TABLE 1**  
General Characteristics of Study Group

Variable	Mean $\pm$ SD
Body mass index (kg/m <sup>2</sup> )	22.5 $\pm$ 3.5
Systolic BP (mm Hg)	116.0 $\pm$ 11.6
Diastolic BP (mm Hg)	71.0 $\pm$ 6.2
Total cholesterol (mmol/L)	5.12 $\pm$ 1.12
HDL cholesterol (mmol/L)	1.52 $\pm$ 0.38
Triglycerides (mmol/L)	0.86 $\pm$ 0.41
HbA <sub>1c</sub> (%)	7.8 $\pm$ 2.6
Insulin (fasting, pmol/L)	48.0 $\pm$ 8.4
WBGDR ( $\mu\text{mol}/\text{min}/\text{kg}$ )	27.2 $\pm$ 12.8

BP = blood pressure; HbA<sub>1c</sub> = hemoglobin A<sub>1c</sub>; HDL = high-density lipoprotein; WBGDR = whole-body GDR.

Before the injection of  $^{18}\text{F}$ -FDG, hyperinsulinemic euglycemic clamping was undertaken to keep the plasma glucose concentration around 100 mg/dL by simultaneous infusion of insulin at a fixed rate (6 pmol/kg/min) and glucose at a variable rate. When the plasma glucose concentration became constant,  $^{18}\text{F}$ -FDG (185–370 MBq) was injected intravenously over 60 s. Dynamic imaging of the midhigh region was started at commencement of tracer injection and continued for 60 min 45 s. Five 15-s frames were acquired, followed by the collection of three 30-s frames, four 120-s frames, four 300-s frames, and three 600-s frames. An arterial blood sample for the measurement of plasma radioactivity was taken at the midtime of each frame during the entire imaging period, and a total of 19 arterial blood samples were obtained. In addition, radioactivity in venous plasma was assayed at the midtime of each frame for the last 7 frames. Arterialization of venous blood was not undertaken.

### Data Analysis

All data were corrected for dead time, decay, and measured photon attenuation, and transaxial images were reconstructed. Fifteen circular regions of interest (ROIs) of 5 mm in diameter were placed within the femoral muscles of each side. Tissue activity was determined from the mean counts for the 30 ROIs and used for the calculation of SMGU, SUV, and SM/B ratio. Arterial plasma and tissue time–activity curves were analyzed by the graphical method described by Patlak et al. (23) to determine the fractional rate of tracer uptake and phosphorylation (K complex [K<sub>i</sub>]). In the graphical analysis, the slope of the linear portion of the plots, which is equal to K<sub>i</sub>, was calculated by linear regression of the last 7 points. K<sub>i</sub> is equal to  $k_1 \times k_3 / (k_2 + k_3)$ , where  $k_1$  is the transfer coefficient from intravascular space into the tissue,  $k_2$  is the initial clearance and efflux coefficient, and  $k_3$  is the phosphorylation rate constant. The dephosphorylation rate constant,  $k_4$ , is assumed to be zero in the Patlak method. SMGU was calculated by substituting K<sub>i</sub> in the equation  $\text{SMGU} = K_i \times \text{GI}_p / \text{LC}$ , where  $\text{GI}_p$  is the mean of the plasma glucose level measured every 5 min during imaging, and LC is the lumped constant. The LC represents the differences in the transport and phosphorylation of  $^{18}\text{F}$ -FDG and glucose and was assumed to be 1.0 in skeletal muscle cells (5,11–20). To calculate SMGU, we used an Ultra 30 high-speed image-processing system (Sun Microsystems Japan) with Dr. View software (Asahi Kasei Information System Co. Ltd.).

The SUV and the SM/B ratio were defined as simple indices of SMGU. SUV was calculated by the equation  $\text{SUV} = (\text{Ct} \times$

BW)/(ID × CF), where Ct is tissue count (counts per second [cps]/mL), BW is body weight (g), and ID is injected dose (MBq). CF is the calibration factor between the dose calibrator and PET. Tissue counts were determined on the last 2 frames of dynamic imaging. The midtime of the last frame was 55.75 min, and the SUV at 55 min was calculated using the tissue count on this frame. The SUV at 45 min was obtained from the next to last frame. The tissue count on the last frame (cps/mL) was divided by venous plasma activity (cps/mL) at the corresponding time, and the SM/B ratio at 55 min was defined. The SM/B ratio at 45 min was calculated in a similar fashion. SMGU was plotted against the SUVs and SM/B ratios, and linear regression analysis was performed. SMGU was estimated using the regression equation thus obtained and the SUV or SM/B ratio and was compared by linear regression with the SMGU measured by Patlak graphical analysis. The residual, absolute difference between measured and estimated SMGUs was calculated as the indicator of estimation error.

Moreover, SUVs and SM/B ratios were corrected for plasma glucose level. The SUVs and SM/B ratios were multiplied by the plasma glucose level (in mg/dL) and divided by 100 to obtain corrected indices. The corrected indices were compared with SMGU, in a manner similar to the uncorrected indices.

### Statistical Analysis

Data are expressed as mean ± SD. Linear regression analysis was performed by the least-squares method. A paired *t* test was used to compare the errors in estimating SMGU. A *P* value < 0.05 was considered significant.

### RESULTS

SMGU was successfully calculated by Patlak graphical analysis in the 10 patients and determined at  $43.8 \pm 29.2$   $\mu\text{mol}/\text{min}/\text{kg}$  (range, 6.5–85.2  $\mu\text{mol}/\text{min}/\text{kg}$ ). A significant negative correlation was found between SMGU and venous plasma activity at 45 min (Fig. 1,  $r = -0.659$ ,  $P < 0.05$ ). The relationship between SMGU and venous plasma activity at 55 min was similar, although it did not reach statistical significance ( $r = -0.632$ ,  $P = 0.05$ ).

SUVs at 45 and 55 min were  $3.22 \pm 1.31$  (range, 1.46–5.79) and  $3.34 \pm 1.40$  (range, 1.45–6.04), respectively. SMGU was highly correlated with SUVs at 45 min (Fig. 2A;  $y = 20.91x - 23.61$ ,  $r = 0.941$ ,  $P < 0.0001$ ) and 55 min ( $y = 19.77x - 22.23$ ,  $r = 0.951$ ,  $P < 0.0001$ ). SM/B ratios at 45 and 55 min were  $1.094 \pm 0.798$  (range, 0.275–2.663) and  $1.304 \pm 0.940$  (range, 0.279–2.970), respectively. There was also an excellent correlation between SMGU and SM/B ratios (Fig. 2B;  $y = 35.42x + 5.02$ ,  $r = 0.968$ , and  $P < 0.0001$  at 45 min;  $y = 30.56x + 3.93$ ,  $r = 0.984$ , and  $P < 0.0001$  at 55 min). The *y*-intercepts of the regression lines for SUVs, but not SM/B ratios, were significantly less than zero ( $P < 0.05$ ). SMGU estimated from these simple indices and the regression equations was highly correlated with the measured SMGU (Fig. 3). The residual was marginally smaller for SM/B ratios than for SUVs and for indices at 55 min rather than at 45 min (Table 2); however, these differences were not statistically significant.

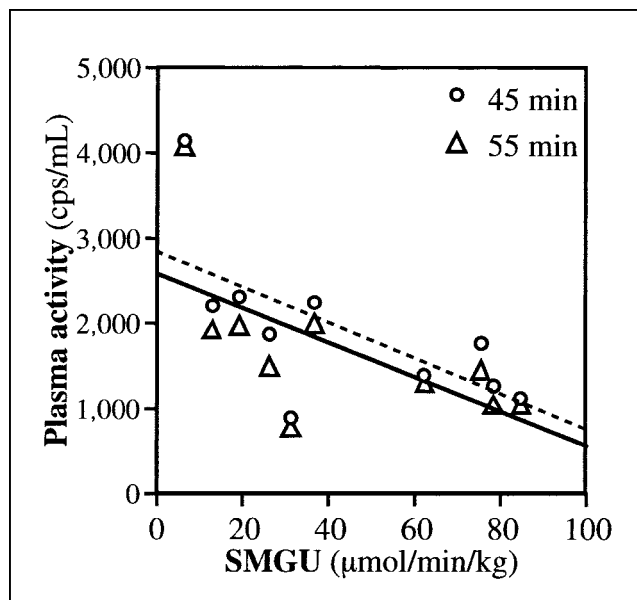


**FIGURE 1.** SMGU and venous plasma activities at 45 and 55 min. Broken and solid lines represent regression lines for plasma activities at 45 min ( $y = -20.9x + 2839.0$ ,  $r = -0.659$ ,  $P < 0.05$ ) and 55 min ( $y = -20.1x + 2591.3$ ,  $r = -0.632$ ,  $P = 0.05$ ), respectively.

Plasma glucose levels during PET ranged from 94 to 120 mg/dL with a mean of  $106 \pm 7$  mg/dL. Plasma insulin levels were  $56.0 \pm 4.2$   $\mu\text{U}/\text{mL}$ . Correction for plasma glucose level slightly elevated the correlation coefficients between SMGU and SUVs (Fig. 4A; 0.966 at 45 min, 0.971 at 55 min) and between SMGU and SM/B ratios (Fig. 4B; 0.982 at 45 min, 0.991 at 55 min). The *y*-intercepts of the regression lines for corrected SUVs were significantly less than zero ( $P < 0.01$ ), but those for SM/B ratios did not significantly differ from zero. Estimation of SMGU from the corrected indices was successful (Fig. 5). The residuals for the corrected indices were smaller than those for the corresponding uncorrected indices; however, the difference was minimal and did not reach statistical significance (Table 2).

### DISCUSSION

The SUVs and SM/B ratios calculated at 45 and 55 min showed excellent correlations with SMGU measured by dynamic PET imaging with frequent arterial blood sampling. The excellent correlations may be related to constant plasma glucose level during hyperinsulinemic euglycemic clamping. The femoral region contains a large amount of skeletal muscle and is away from other tissues with high  $^{18}\text{F}$ -FDG uptake, which may have also contributed to the successful results. A mean SMGU value in healthy subjects has been reported as 108.9  $\mu\text{mol}/\text{min}/\text{kg}$  (20), and the population in this study is considered to include patients with insulin resistance. The results of this study indicate that SUVs and SM/B ratios can be used as simple quantitative indices of SMGU to assess insulin resistance. The SUV is

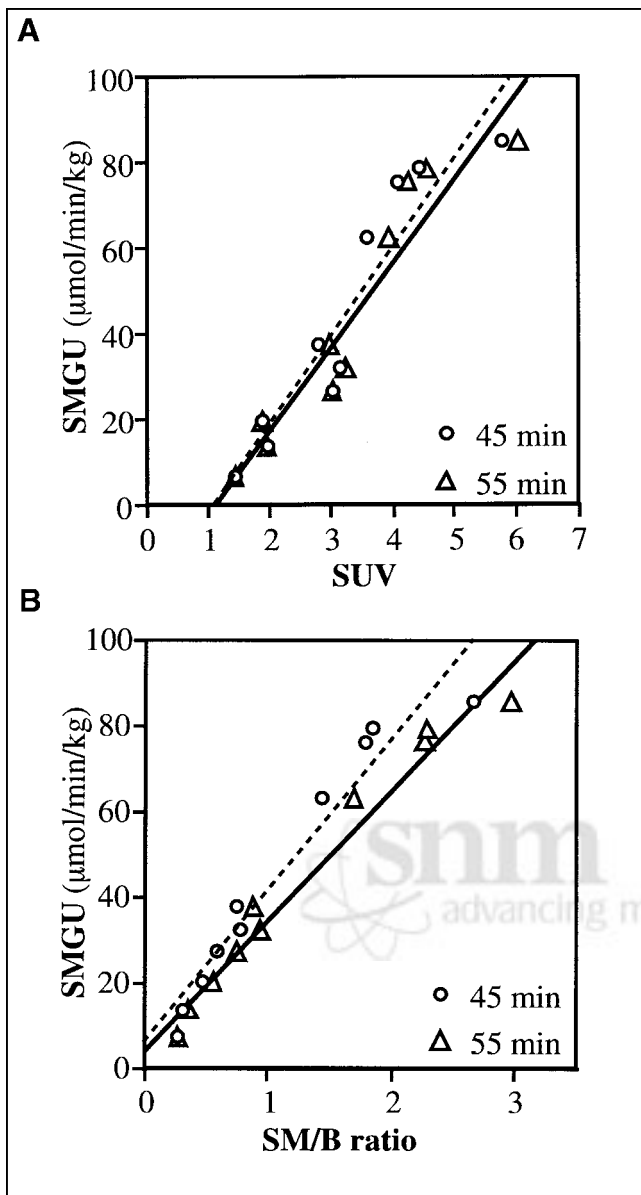


**FIGURE 2.** Relation between SMGU and simple indices. (A) SMGU vs. SUV. Broken and solid lines represent regression lines for SUVs at 45 min ( $y = 20.91x - 23.61$ ,  $r = 0.941$ ,  $P < 0.0001$ ) and 55 min ( $y = 19.77x - 22.23$ ,  $r = 0.951$ ,  $P < 0.0001$ ), respectively. (B) SMGU vs. SM/B ratio. Broken and solid lines represent regression lines for SM/B ratios at 45 min ( $y = 35.42x + 5.02$ ,  $r = 0.968$ ,  $P < 0.0001$ ) and 55 min ( $y = 30.56x + 3.93$ ,  $r = 0.984$ ,  $P < 0.0001$ ), respectively.

obtained using static imaging, and the SM/B ratio is derived from static imaging and a single venous blood sampling. Use of these indices allows shortening of imaging time and omission of frequent arterial blood sampling and facilitates the evaluation of insulin resistance in clinical settings. We experienced substantial body movement during dynamic imaging in 1 subject of this series. A reliable tissue time-activity curve could not be obtained, resulting in failure in calculating SMGU by the Patlak graphical method. These data were excluded from the analysis because of the lack of

a standard value; however, the SUV and SM/B ratio could be computed as indicators of SMGU in this case. Imaging of the extremities is susceptible to degradation due to patient motion. Reduction of imaging time appears to decrease the frequency of failure to collect reliable data.

The SUV and SM/B ratio can be converted to SMGU with empiric equations determined in this study. The relation between SMGU and the simple indices does not appear to largely depend on the performance of the equipment

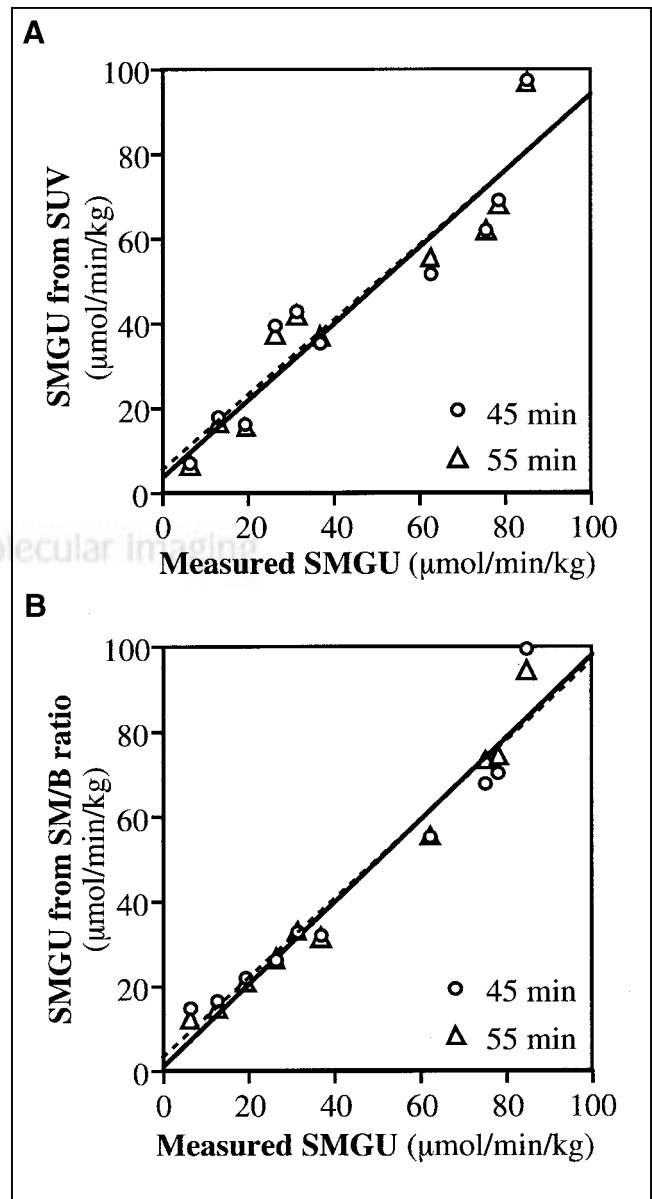


**FIGURE 3.** Relation between SMGUs measured by Patlak graphical analysis and estimated from simple indices. (A) Estimation from SUV. Broken and solid lines represent regression lines for SUVs at 45 min ( $y = 0.886x + 4.98$ ,  $r = 0.941$ ) and 55 min ( $y = 0.904x + 4.22$ ,  $r = 0.951$ ), respectively. (B) Estimation from SM/B ratio. Broken and solid lines represent regression lines for SM/B ratios at 45 min ( $y = 0.937x + 2.75$ ,  $r = 0.968$ ) and 55 min ( $y = 0.969x + 1.35$ ,  $r = 0.984$ ), respectively.

**TABLE 2**  
Residual in Estimating SMGU from Simple Indices

Index	Residual	
	Correction (-)	Correction (+)
SUV at 45 min	8.1 ± 5.0	5.7 ± 4.6
SUV at 55 min	7.2 ± 5.0	4.7 ± 4.9
SM/B ratio at 45 min	5.7 ± 4.1	4.2 ± 3.2
SM/B ratio at 55 min	3.9 ± 3.1	3.2 ± 1.9

Index = simple index used for estimation of SMGU; Correction (-) = without correction for plasma glucose level; Correction (+) = with correction for plasma glucose level.

Data are presented as mean ± SD.

used. The equations are inferred to be applicable in other laboratories, although validation is desired. Conversion to SMGU appears to aid in comparing the obtained values with SMGU reported in other studies. The simple indices are obtained by imaging of relatively short duration, and sequential imaging at different positions may allow assessment of  $^{18}\text{F}$ -FDG uptake in different regions. For example, SMGU in the trunk may be calculated from the SUV or SM/B ratio at 45 min and in the femoral region from the SUV or SM/B ratio at 55 min. The SUV at 55 min is higher than that at 45 min due to gradual uptake by the skeletal muscle. The time-dependent difference is larger for the SM/B ratio than for the SUV because of plasma clearance. Conversion to SMGU corrects such systematic difference, as shown in Figures 3 and 5, and appears to be useful for the direct comparison of values derived from imaging at different time intervals. Estimation of SMGU in different regions after a single injection of  $^{18}\text{F}$ -FDG permits the analysis of regional differences in SMGU and may offer a unique viewpoint on insulin resistance.

Although SM/B ratios were almost proportional to SMGU, the  $y$ -intercepts of the regression lines between SUVs and SMGU significantly differed from zero. The basis of using the SUV as an indicator of  $^{18}\text{F}$ -FDG uptake is the assumption that the injected dose normalized for body weight represents the input function. Skeletal muscles take up the majority of glucose during insulin stimulation in healthy subjects (29). A higher SMGU may induce faster plasma clearance of  $^{18}\text{F}$ -FDG and, consequently, decreased input at the same injected dose normalized for body weight, leading to underestimation of SMGU by using SUV. In this study, SMGU and plasma activity at the late phase were negatively correlated, supporting the effect of SMGU on plasma clearance of  $^{18}\text{F}$ -FDG. In calculating SM/B ratios, venous plasma activity at static imaging is used instead of the injected dose normalized for body weight. The proportionality between the SM/B ratio and SMGU indicates that venous plasma activity at a late phase is a useful marker of input function. Correlation coefficients between SMGU and SM/B ratios were slightly higher than those between SMGU

and SUVs. The residual in estimating SMGU was smaller using SM/B ratios than when using SUVs, but the difference was not statistically significant. Only a small number of patients were examined in this study, and further investigation of a larger population appears to be required to determine which index is better for assessing SMGU. However, it should be noted that the SUV is not proportional to

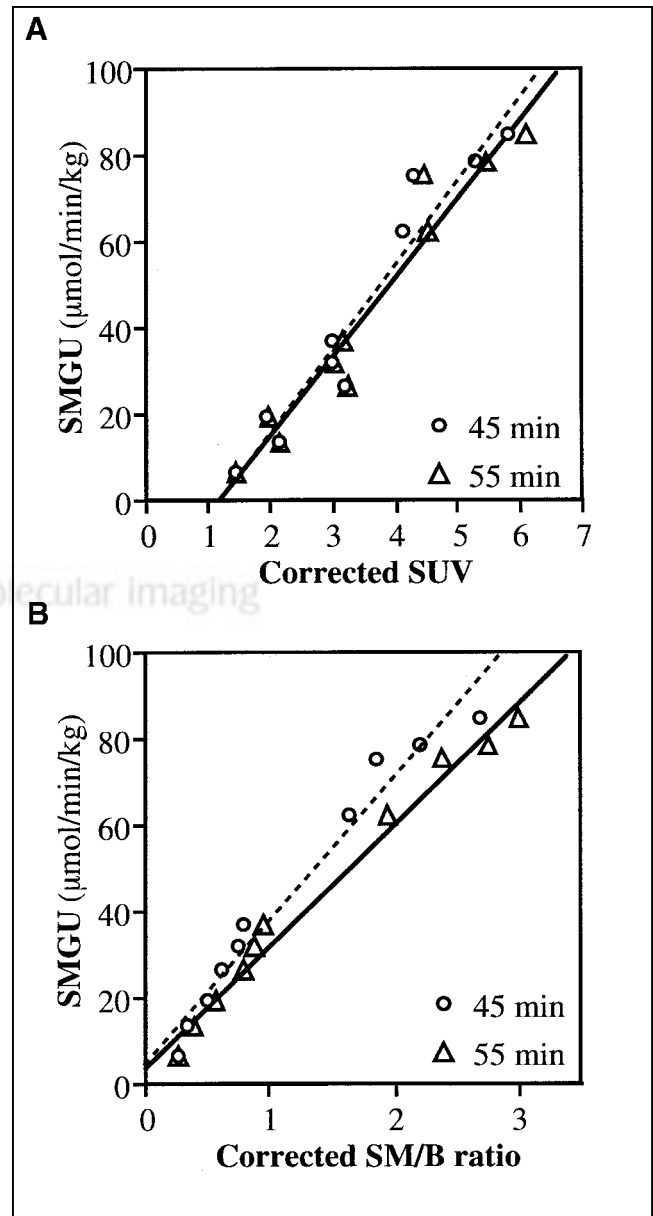


**FIGURE 4.** Relation between SMGU and simple indices corrected for plasma glucose level. (A) SMGU vs. corrected SUV. Broken and solid lines represent regression lines for corrected SUVs at 45 min ( $y = 19.57x - 23.47$ ,  $r = 0.966$ ,  $P < 0.0001$ ) and 55 min ( $y = 18.39x - 21.74$ ,  $r = 0.971$ ,  $P < 0.0001$ ), respectively. (B) SMGU vs. corrected SM/B ratios. Broken and solid lines represent regression lines for SM/B ratios at 45 min ( $y = 33.32x + 4.70$ ,  $r = 0.982$ ,  $P < 0.0001$ ) and 55 min ( $y = 28.25x + 4.23$ ,  $r = 0.991$ ,  $P < 0.0001$ ), respectively.

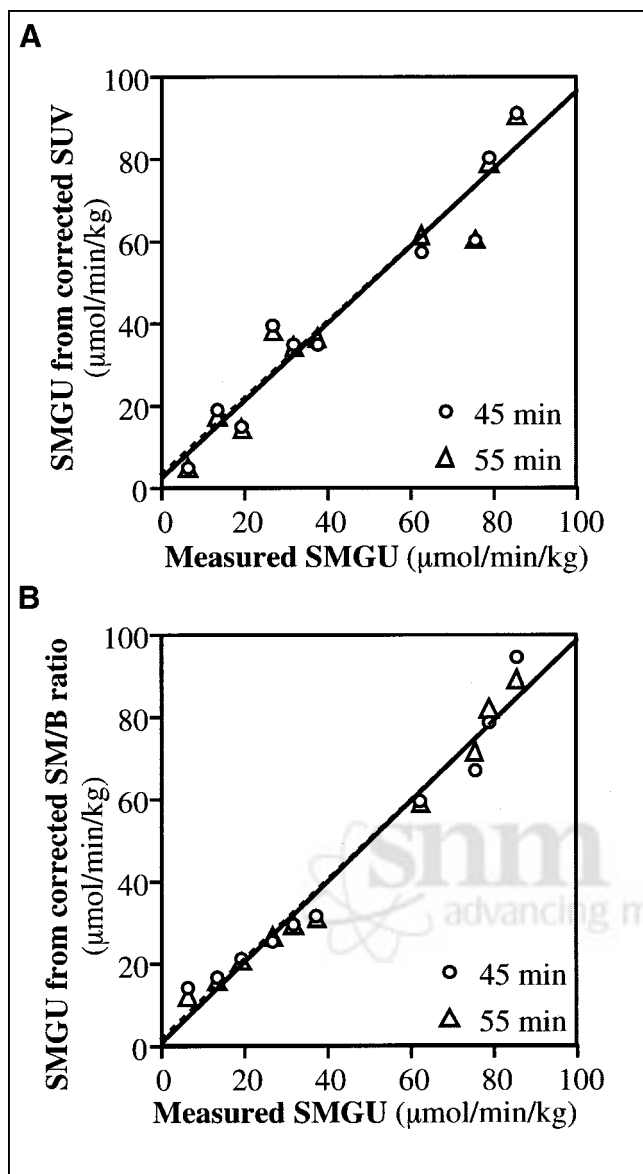


**FIGURE 5.** Relation between SMGUs measured by Patlak graphical analysis and estimated from simple indices corrected for plasma glucose level. (A) Estimation from corrected SUV. Broken and solid lines represent regression lines for corrected SUVs at 45 min ( $y = 0.932x + 2.96$ ,  $r = 0.966$ ) and 55 min ( $y = 0.943x + 2.49$ ,  $r = 0.971$ ), respectively. (B) Estimation from corrected SM/B ratio. Broken and solid lines represent regression lines for corrected SM/B ratios at 45 min ( $y = 0.965x + 1.54$ ,  $r = 0.982$ ) and 55 min ( $y = 0.983x + 0.76$ ,  $r = 0.991$ ), respectively.

SMGU during insulin clamping, and conversion to SMGU seems to be recommendable especially for SUV.

The SUV is considered to be an approximate of the Patlak slope,  $K_i$  (30), as is the SM/B ratio. Fundamentally, they should be corrected for the plasma glucose level when making comparisons with SMGU. In this study, correction for the plasma glucose level did improve the correlation between these simple indices and SMGU and decreased residuals in estimating SMGU. The differences, however,

were insignificant. Lack of statistical significance may be partly attributable to the small population studied. In addition, it appears to be related to the fact that SMGU was evaluated during hyperinsulinemic euglycemic clamping. Interexamination variation in the plasma glucose level was small, and the correction did not cause a large difference in estimated values. On the other hand, the plasma glucose level is monitored in insulin clamping, and the correction does not add substantial labor. Thus, correcting for the plasma glucose level would be recommended, although the effect is minimal.

The results of this study indicate the usefulness of SUVs and SM/B ratios in evaluating SMGU during hyperinsulinemic euglycemic clamping. The applicability remains to be investigated in the fasting or postprandial state. The use of simple indices has been considered in cardiac studies. Tamaki et al. suggested that the  $^{18}\text{F}$ -FDG uptake index, an analog of SUV, could be used as an indicator of MGU in the fasting state but not in the postprandial state (26). They ascribed the failure to temporal changes in plasma glucose and insulin levels during the examination. They correlated the  $^{18}\text{F}$ -FDG uptake index to MGU without correction for the plasma glucose level, which may also be related to the failure. Choi et al. found a good correlation between  $K_i$  and normalized myocardial  $^{18}\text{F}$ -FDG uptake, which is also analogous to SUV, in both fasting and postprandial states (31). Nishikawa et al. reported that the  $^{18}\text{F}$ -FDG uptake index and M/B ratio can be used as indicators of  $K_i$  for the myocardium during fasting, oral glucose loading, and insulin clamping (27). The SUV and SM/B ratio may also reflect SMGU in the fasting and postprandial states as well as during insulin clamping, and correction for plasma glucose level appears to be necessary for diabetic and postprandial patients.

## CONCLUSION

The results of this study indicate that SMGU can be estimated using the simple quantitative indices, SUVs and SM/B ratios, during hyperinsulinemic euglycemic clamping. Evaluation of SMGU by static  $^{18}\text{F}$ -FDG PET might be of value in investigations of insulin resistance.

## ACKNOWLEDGMENTS

We thank Tohru Inoue and Yoshio Kojima for their technical support in preparing  $^{18}\text{F}$ -FDG.

## REFERENCES

- DeFronzo RA, Gunnarsson R, Bjorkman O, et al. Effect of insulin on peripheral and splanchnic glucose metabolism in non-insulin dependent (type II) diabetes mellitus. *J Clin Invest.* 1985;76:149–155.
- Steiner G, Morita S, Vranic M. Resistance to insulin but not to glucagon in lean human hypertriglyceridemics. *Diabetes.* 1980;29:899–905.
- Reaven GM, Mejean L, Villaume C, Drouin P, Debry G. Plasma glucose and insulin responses to oral glucose in nonobese subjects and patients with endogenous hypertriglyceridemia. *Metabolism.* 1983;32:447–450.
- Yki-Jarvinen H, Taskinen MR. Interrelationships among insulin's antilipolytic and glucoregulatory effects and plasma triglycerides in nondiabetic and diabetic patients with endogenous hypertriglyceridemia. *Diabetes.* 1988;37:1271–1278.

5. Nuutila P, Maki M, Laine H, et al. Insulin action on heart and skeletal muscle glucose uptake in essential hypertension. *J Clin Invest.* 1995;96:1003–1009.
6. Reaven GM. Banting lecture 1988: role of insulin resistance in human disease. *Diabetes.* 1988;37:1595–1607.
7. DeFronzo RA. Insulin resistance, hyperinsulinemia, and coronary artery disease: a complex metabolic web. *J Cardiovasc Pharmacol.* 1992;20(suppl 11):S1–S16.
8. Laakso M, Edelman SV, Brechtel G, Baron AD. Decreased effect of insulin to stimulate skeletal muscle blood flow in obese man: a novel mechanism for insulin resistance. *J Clin Invest.* 1990;85:1844–1852.
9. Roden M, Price TB, Perseghin G, et al. Mechanism of free fatty acid-induced insulin resistance in humans. *J Clin Invest.* 1996;97:2859–2865.
10. Boden G. Fatty acids and insulin resistance. *Diabetes Care.* 1996;19:394–395.
11. Nuutila P, Koivisto VA, Knuuti J, et al. Glucose-free fatty acid cycle operates in human heart and skeletal muscle in vivo. *J Clin Invest.* 1992;89:1767–1774.
12. Voipio-Pulkki LM, Nuutila P, Knuuti MJ, et al. Heart and skeletal muscle glucose disposal in type 2 diabetic patients as determined by positron emission tomography. *J Nucl Med.* 1993;34:2064–2067.
13. Nuutila P, Raitakari M, Laine H, et al. Role of blood flow in regulating insulin-stimulated glucose uptake in humans: studies using bradykinin, [<sup>15</sup>O]water, and [<sup>18</sup>F]fluoro-deoxy-glucose and positron emission tomography. *J Clin Invest.* 1996;97:1741–1747.
14. Paternostro G, Camici PG, Lammerstma AA, et al. Cardiac and skeletal muscle insulin resistance in patients with coronary heart disease: a study with positron emission tomography. *J Clin Invest.* 1996;98:2094–2099.
15. Kelley DE, Mintun MA, Watkins SC, et al. The effect of non-insulin-dependent diabetes mellitus and obesity on glucose transport and phosphorylation in skeletal muscle. *J Clin Invest.* 1996;97:2705–2713.
16. Raitakari M, Nuutila P, Ruotsalainen U, et al. Evidence for dissociation of insulin stimulation of blood flow and glucose uptake in human skeletal muscle: studies using [<sup>15</sup>O]H<sub>2</sub>O, [<sup>18</sup>F]fluoro-2-deoxy-D-glucose, and positron emission tomography. *Diabetes.* 1996;45:1471–1477.
17. Yokoyama I, Ohtake T, Momomura S, et al. Organ-specific insulin resistance in patients with noninsulin-dependent diabetes mellitus and hypertension. *J Nucl Med.* 1998;39:884–889.
18. Laine H, Yki-Jarvinen H, Kirvela O, et al. Insulin resistance of glucose uptake in skeletal muscle cannot be ameliorated by enhancing endothelium-dependent blood flow in obesity. *J Clin Invest.* 1998;101:1156–1162.
19. Ronnema EM, Ronnema T, Utriainen T, et al. Decreased blood flow but unaltered insulin sensitivity of glucose uptake in skeletal muscle of chronic smokers. *Metabolism.* 1999;48:239–244.
20. Yokoyama I, Yonekura K, Moritan T, et al. Troglitazone improves whole-body insulin resistance and skeletal muscle glucose use in type II diabetic patients. *J Nucl Med.* 2001;42:1005–1010.
21. Reinhardt M, Beu M, Vosberg H, et al. Quantification of glucose transport and phosphorylation in human skeletal muscle using FDG PET. *J Nucl Med.* 1999;40:977–985.
22. Lackner R, Challiss RA, West D, Newsholme EA. A problem in the radiochemical assay of glucose-6-phosphatase in muscle. *Biochem J.* 1984;218:649–651.
23. Patlak CS, Blasberg RG, Fenstermacher JD. Graphical evaluation of blood-to-brain transfer constants from multiple-time uptake data. *J Cereb Blood Flow Metab.* 1983;3:1–7.
24. Weber WA, Schwaiger M, Avril N. Quantitative assessment of tumor metabolism using FDG-PET imaging. *Nucl Med Biol.* 2000;27:683–687.
25. Tashiro M, Fujimoto T, Itoh M, et al. <sup>18</sup>F-FDG PET imaging of muscle activity in runners. *J Nucl Med.* 1999;40:70–76.
26. Tamaki N, Yonekura Y, Kawamoto M, et al. Simple quantification of regional myocardial uptake of fluorine-18-deoxyglucose in the fasting condition. *J Nucl Med.* 1991;32:2152–2157.
27. Nishikawa J, Ohtake T, Yokoyama I, Watanabe T, Momose T, Sasaki Y. Simple method to quantify myocardial glucose metabolism from MB ratio in myocardial FDG PET. *Ann Nucl Med.* 1996;10:323–328.
28. Ehrenkauffer RE, Potocki JF, Jewett DM. Simple synthesis of F-18-labeled 2-fluoro-2-deoxy-D-glucose: concise communication. *J Nucl Med.* 1984;25:333–337.
29. DeFronzo RA, Jacot E, Jequier E, Maeder E, Wahren J, Felber JP. The effect of insulin on the disposal of intravenous glucose: results from indirect calorimetry and hepatic and femoral venous catheterization. *Diabetes.* 1981;30:1000–1007.
30. Thie JA. Clarification of a fractional uptake concept [letter]. *J Nucl Med.* 1995;36:711–712.
31. Choi Y, Brunken RC, Hawkins RA, et al. Factors affecting myocardial 2-[F-18]fluoro-2-deoxy-D-glucose uptake in positron emission tomography studies of normal humans. *Eur J Nucl Med.* 1993;20:308–318.

